ΩInt. J. Electrochem. Sci., 8 **(2013)** 7656 - 7668

International Journal of
ELECTROCHEMICAL
SCIENCE
www.electrochemsci.org

Positron Annihilation Spectroscopy and Electrochemical Impedance Spectroscopy Studies of Polyurethane-Urea Hybrid Coatings

Mara Cristina Lopes de Oliveira[1], *Renato Altobelli Antunes*[2,*], *Isolda Costa*[3]

[1]Electrocell Ind. Com. Equip. Elet. LTDA, Technology, Entrepreneurship and Innovation Center (CIETEC), 05508-000 São Paulo-SP, Brazil
[2] Engineering, Modeling and Applied Social Sciences Center (CECS), Federal University of ABC (UFABC), 09210-170, Santo André-SP, Brazil
[3] IPEN/CNEN-SP, Av. Prof. Lineu Prestes 2242, 05508-000, São Paulo, SP, Brazil
[*]E-mail: renato.antunes@ufabc.edu.br

Received: 18 April 2013 / *Accepted:* 14 May 2013 / *Published:* 1 June 2013

The aim of this work was to study the physical aging behavior and corrosion resistance of polyurethane-urea hybrid coatings by positron annihilation spectroscopy and electrochemical impedance spectroscopy (EIS). Two coatings with different NCO/OH ratios have been prepared using the pre-polymer method. The coatings structure was characterized by Fourier transform-infrared spectroscopy. Differential scanning calorimetry (DSC) was used as a complimentary technique to evaluate the physical aging behavior of the coatings. The results showed that the coatings were only little affected by physical aging and presented high corrosion resistance. However, the coating with the highest NCO/OH presented the best general performance. The results obtained by positron annihilation spectroscopy and EIS were in good agreement, suggesting that there is a direct relationship between the physical aging and corrosion behavior of the coatings prepared in this work.

Keywords: positron annihilation; polyurethane-urea hybrid coating; physical aging; EIS; corrosion

1. INTRODUCTION

Protective organic coatings can be degraded by environmental factors such as humidity, temperature, oxygen and light [1]. Corrosion protection of metallic materials by organic coatings is based on the barrier action for ions, adhesion to the substrate and presence of active pigments or inhibitors which are released when the coating layer is damaged [2]. Stratmann et al. [3] showed that the barrier properties of intact polymeric films are hampered by the diffusion of water and oxygen. The

diffusion of water molecules at the metal/coating interface can deteriorate the film adhesion to substrate, facilitating the onset of corrosion underneath the organic layer [4].

Electrochemical impedance spectroscopy (EIS) is a powerful non-destructive technique widely employed to investigate the protective performance of organic coatings [5,6]. It is based on the measurement of the current response on small sinusoidal perturbations of the electrode potential as a function of the frequency of the signal [7]. The impedance response of the metal/coating system is associated with its corrosion resistance [8]. When interpreting EIS data through Bode modulus plots, a high performance coating with good barrier properties is recognized by the formation of a straight line with unit negative slope which indicates a pure capacitive behavior. Corrosion processes associated with water diffusion through the coating thickness would cause the modulus of impedance to deviate from this straight line path. Organic coatings which demonstrate good barrier properties are frequently reported to have a modulus of impedance exceeding 10^7 $\Omega.cm^2$ at low frequencies [9,10].

Slow positrons have been used to fundamental and applied research concerning bulk properties of organic coatings. Change in local free volume properties due to environmental factors can be readily evaluated using slow positrons, giving information on the physical aging of polymeric films [11]. Positron annihilation spectroscopy experiments can be performed by Doppler broadening of energy spectra (DBES) or positron annihilation lifetime (PAL) measurements. In DBES experiments the momentum distribution around the 511 keV energy peak is monitored. The obtained spectrum is characterized by the so-called S parameter which is the ratio of integrated counts in the central part of the peak to the total counts after the background is subtracted. The main factors that contribute to the S parameter in polymers are free-volume content, free-volume size and composition. The S parameter is a direct measure of the quantity of momentum dispersion. A decrease of the S value is associated with loss of free-volume [12]. Some authors have reported that positron annihilation spectroscopy and corrosion studies of organic coatings are correlated, since the distribution of free-volume in the polymeric structure is strictly related to its water uptake ability and barrier properties [13,14].

Physical aging, a relaxation process of organic coatings resulting from their non-equilibrium state, affect mechanical, thermal, electrical and transport (diffusion and permeability) properties [15]. The free-volume distribution changes during physical aging. Thus, it is possible to assess the susceptibility of organic coatings to this phenomenon using experimental techniques which are capable of quantifying parameters related to free-volume changes. In this regard, the S parameter determined by positron annihilation spectroscopy can be used to study the physical aging of organic coatings. Differential scanning calorimetry (DSC) is also traditionally employed to investigate the physical aging behavior of organic films. The variation of enthalpy determined from DSC curves is directly related to the susceptibility of the organic film to this phenomenon [16].

Polyurethane-urea hybrid coatings with low volatile organic compounds (VOCs) have been considered as alternatives to conventional polyurethane coatings due to improved mechanical properties and barrier performance [17]. Restrictive regulations towards the reduction of VOC emissions have driven the development of water-based and high solids coatings [18]. Polyurethane-based coatings play a major part in this scenario [19]. Although positron annihilation spectroscopy studies of polyurethane-based coatings have been previously reported [20,21], studies concerning polyurethane-urea hybrid coatings have not been reported. The aim of this work was to use positron

annihilation spectroscopy experiments based on DBES to examine the physical aging behavior of two polyurethane-urea hybrid coatings with different NCO/OH mole ratios. DSC measurements were also performed as a complimentary method of evaluating the physical aging behavior of the hybrid films. Moreover, the corrosion performance of the coatings was assessed by electrochemical impedance spectroscopy in order to investigate how the physical aging and corrosion behavior are correlated.

2. MATERIALS AND METHODS

2.1 Materials

Commercial grades of toluene diisocyanate (TDI, a mixture of 80% 2,4-TDI and 20% 2,6-TDI) and polytetramethylene glycol (PTMEG; molecular weight = 1000 $g.mol^{-1}$) were supplied by Basf. Ethylene diamine (EDA, supplied by Coremal Brasil) was used as both curing agent and chain extender. The coatings produced in this work are 100% solid films and, thus, no solvents were used in the synthesis process.

2.2 Preparation of the polyurethane-urea hybrid coatings

A two-component polyurethane-urea hybrid coating was prepared. Component A was prepared using the traditional pre-polymer method. First, a NCO-terminated pre-polymer was prepared by carrying out the reaction in a 500 mL three necked round bottom flask equipped with a thermometer, dropping funnel and by continuously purging with nitrogen flow. The reaction was conducted over a digital magnetic heating/stirrer instrument. Initially, a fixed weight of PTMEG was heated at 45 ºC to melt inside the round bottom flask. TDI was added drop-wise through a dropping funnel to the flask at 60 ºC and the addition was continued for 30–40 min. After complete addition, the reaction was carried out for another 2 h at 70 ºC. Meanwhile, component B was prepared by mixing proper quantities of PTMEG and EDA. Next, the reaction was completed by adding the PTMEG/EDA blend to the pre-polymer at specific concentrations to produce polyurethane-urea hybrid coatings with NCO/OH mole ratios of 1.0 (designated as $T_{1.0}$) and 2.0 (designated as $T_{2.0}$).

2.3 Characterization techniques

2.3.1 Positron annihilation spectroscopy

The positrons were generated with 0.012 mCi ($4.5x10^5$ Bq) ^{22}Na source. The DBES spectra were recorded using two HPGeOrtec detectors, analog-to-digital converters (ADC-OrtecAD413), a spectroscopy amplifier (Ortec673), a fast-filter amplifier (FFA-Ortec579), a constant fraction discriminator (CFD-Ortec584), a custom-built CAMAC-to-PC controller (Multi), and a computer system. A detailed description of the experimental procedure can be found in [22]. The duration of each measurement was 180 s. Samples of the $T_{1.0}$ and $T_{2.0}$ coatings were aged at 100 ºC in a kiln under

static air for 24 h and 72 h. Samples of the coatings in the as-prepared condition were also evaluated for comparison. The results are presented as values of the S parameter (shape parameter) and plots of counts as a function of the positron energy. A decrease of the S value is associated with loss of coating flexibility due to reduction of free-volume which can indicate deterioration of coating durability [23].

2.3.2 Differential scanning calorimetry (DSC)

Samples of the different coatings were aged in a kiln at 100 ºC for 24 h and 72 h under static air. Samples of the coatings in the as-prepared condition were also evaluated for comparison. The physical aging behavior of each sample was investigated using DSC. The measurements were carried out in a Shimadzu DSC60 equipment at a heating rate of 10 ºC.min^{-1} from 30 ºC to 380 ºC under synthetic air.

2.3.3 Fourier transform-infrared spectroscopy (FTIR)

FTIR spectra of the different coatings were recorded on Shimadzu FTIR8201PC spectrometer. The samples for the FTIR analysis were translucent films casted onto glass plates before curing. After curing, the films were removed from the plate and submitted to the FTIR analysis. The spectra were determined over the range of 4000-400 cm^{-1} with a resolution setting of 4 cm^{-1}.

2.3.4 Electrochemical impedance spectroscopy (EIS)

The corrosion behavior of the different coatings was assessed using EIS. The measurements were performed in a frequency response analyser Solatron 1255 coupled to a potentiotat/galvanostat (EG&G model 273A). The tests were conducted using a three-electrode cell set-up with a platinum wire as the auxiliary electrode, a standard calomel electrode (SCE) as reference and polyuretnane-urea coated-Al 5451 samples as the working electrodes. The chemical composition of the Al 5451 alloy is given in Table 1. The electrolyte was a naturally aerated NaCl 3.5 wt.% solution at room temperature. The measurements were performed in potentiostatic mode and at the corrosion potential (E_{corr}). The amplitude of the perturbation signal was 10 mV, and the investigated frequency range varied from 50 kHz to 2 Hz with an acquisition rate of 6 points per decade. The electrochemical behaviour was evaluated for up to 42 days of immersion.

Table 1. Chemical composition of the Al 5451 alloy.

	Si	Fe	Cu	Mn	Mg	Cr	Ni	Zn	Al
Mass (%)	0.050	0.190	0.009	0.030	2.050	0.220	0.003	0.009	Balance

Capacitance variation with frequency during EIS measurements can be used to evaluate the performance of organic coatings with regard to water uptake [24]. The capacitance of an organic film increases when it absorbs water [25]. In this work, the capacitance values were determined based on the model used by Castela et al. [26]. The capacitance values are calculated using equation (1), where C is the capacitance, f is the frequency and Z" is the imaginary impedance value at each specific frequency.

$$C = 1/2\pi fZ'' \quad (1)$$

When the capacitance is plotted versus the frequency employed in the EIS measurements it is possible to verify the trend of a limiting capacitance value as the frequency increases. An approximately constant capacitance value may be determined. This stable value can be used as a reference to compare the water absorption ability of different coatings at specific immersion periods. In this work the reference capacitance value corresponded to a frequency of 23 kHz.

3. RESULTS AND DISCUSSION

3.1 FTIR spectra

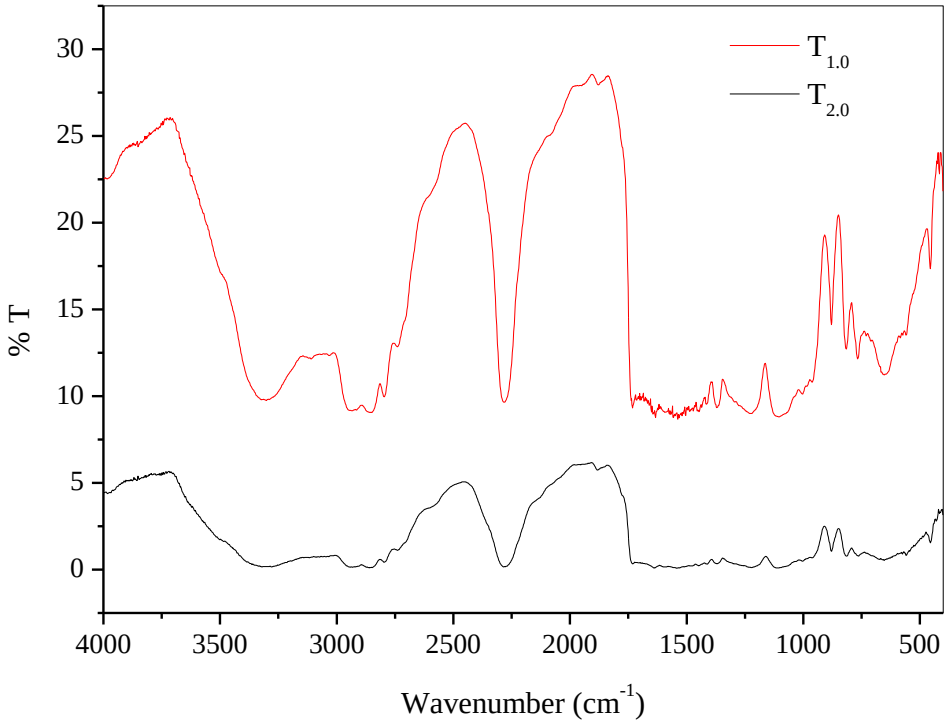

Figure 1. FTIR spectra of the $T_{1.0}$ and $T_{2.0}$ films.

FTIR spectra of the $T_{1.0}$ and $T_{2.0}$ films are shown in Fig. 1. It is possible to observe bands associated with the stretching of N-H of urethane at 3300 cm^{-1} in both coatings [27]. The bands at 1100

cm^{-1} and 1220 cm^{-1} can be attributed to C-O vibrations of ester and ether groups present in the polymer structure. The intense band around 2270 cm^{-1} is typical of non-reacted –NCO [28] and appears in the spectra of both films. In the region between 1600 cm^{-1} and 1750 cm^{-1} weak bands attributed to stretching vibrations of urea (NH-(C=O)) and carbonyl groups can be found in both spectra. Typical vibrations of TDI aromatic ring around 900 cm^{-1} can be found in both spectra [29].

3.2 Positron annihilation spectroscopy

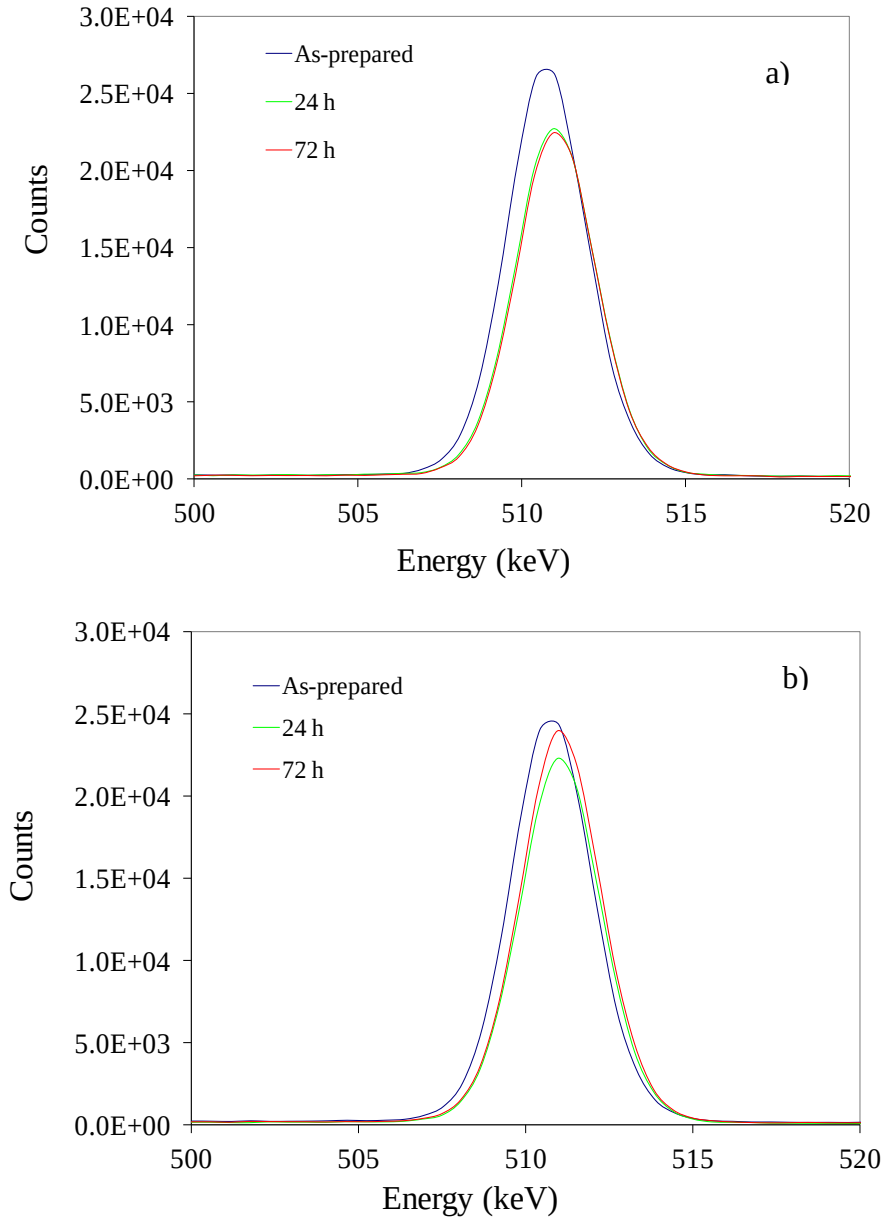

Figure 2. DBES spectra obtained by positron annihilation spectroscopy of the polyurethane-urea coatings in the as-prepared condition and after aging at 100 ºC for 24 h and 72 h under static air: a) $T_{1.0}$; b) $T_{2.0}$.

Figure 2 shows the DBES spectra obtained for the $T_{1.0}$ and $T_{2.0}$ coatings in the as-prepared condition and after aging at 100 ºC for 24 h and 72 h. Values of the S parameter have been determined from these spectra following the procedure described in [30]. It is defined as the ratio of the central part of the DBES spectrum to the total area of the spectrum after the background is properly subtracted. The results are shown in Fig. 3 where the S parameter is plotted as a function of the aging time at 100 ºC for the $T_{1.0}$ and $T_{2.0}$ coatings. Values for the samples of the coatings in the as-prepared condition are also included for comparison.

The results indicate that the S parameter decreased for both coatings after aging at 100 ºC. This behavior suggests that the free volume of the coatings diminishes with aging which is likely to be due to loss of flexibility. Cao et al. [31] reported a similar trend for polyurethane coatings exposed to ultraviolet irradiation. The decrease of the S parameter was associated with photodegradation of the coating with the formation of subnanometer defects and reduction of free volume and holes due to the increasing crosslinking by ultraviolet radiation. In this regard, the results reported in the present work reveal that the polyurethane-urea coatings are prone to physical aging upon heating and this could be promptly assessed by positron annihilation spectroscopy. The values of the S parameter decreased more sharply for the $T_{2.0}$ coating. The value after 72 h of aging at 100 ºC was reduced 19.3% when compared to the value of the as-prepared film.

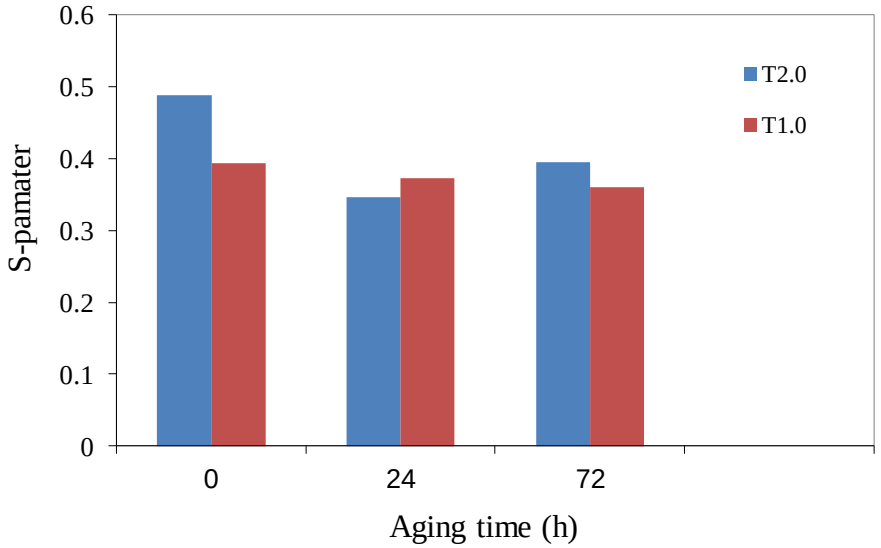

Figure 3. S parameter plotted as a function of the aging time at 100 ºC for the $T_{1.0}$ and $T_{2.0}$ coatings.

For the $T_{1.0}$ coating the reduction was of only 8.3%. This would imply that the $T_{2.0}$ coating, which has a NCO/OH ratio of 2.0, is more prone to physical aging than the $T_{1.0}$ coating which has a NCO/OH of 1.0. However, it is noteworthy that the absolute value of the S parameter is lower after 72 h for the $T_{1.0}$ coating, thus suggesting that a lower NCO/OH would make the organic film more prone to physical aging. In fact, the increase of the NCO/OH ratio in the pre-polymer is expected to improve the resistance of polyurethane-based polymer to physical aging [32]. Hence, if, in one hand, the $T_{2.0}$ coating presented the highest relative reduction of the S parameter with aging time, on the other hand it

also presented the highest absolute value of the S parameter in the peak aged condition. In order to gain a deep understanding on this phenomenon for the coatings examined in the present work, DSC measurements were also performed to evaluate their physical aging behavior.

3.3 Differential scanning calorimetry (DSC)

The quantification of the physical aging susceptibility of organic films through DSC measurements is based on the enthalpy relaxation (endothermic peak) that represents the decrease of enthalpy (ΔH) during aging as the sample is heated after being aged. The value of ΔH which is associated with the neat endothermic peak area can be easily determined using the software that controls the DSC equipment. If the endothermic peak area increases with the aging time, the coating is susceptible to physical aging [33]. DSC curves (heat flow versus temperature) of the $T_{1.0}$ and $T_{2.0}$ coatings heated at 100 ºC for different aging times are shown in Fig.4.

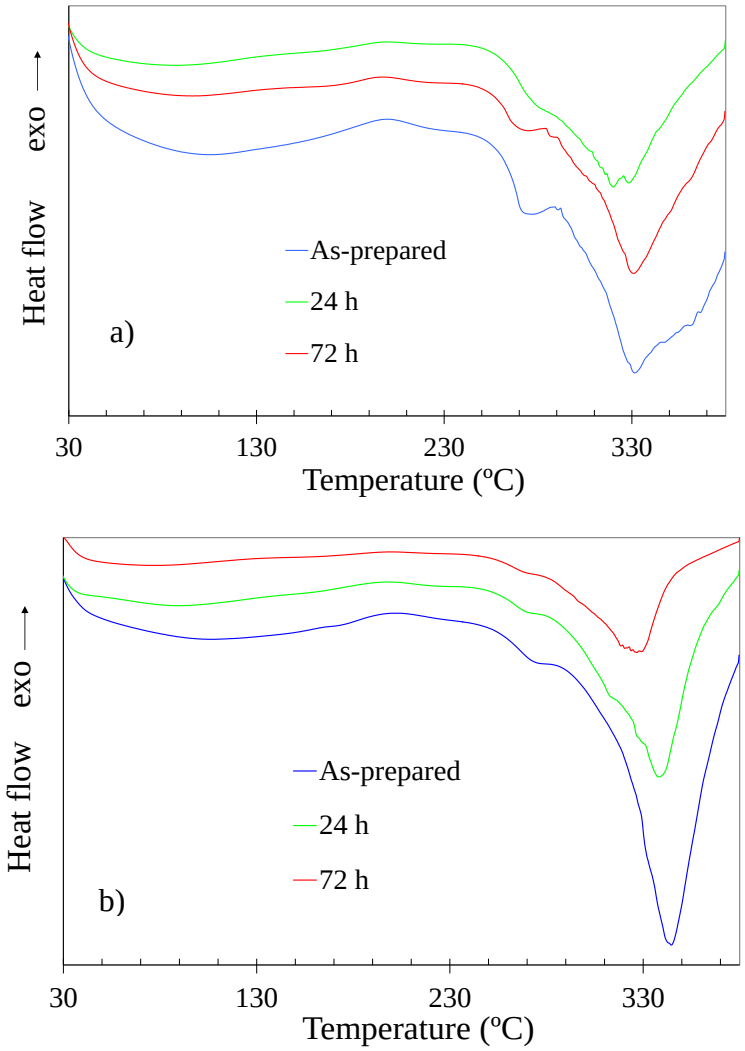

Figure 4. DSC curves (heat flow versus temperature) of the polyurethane-urea coatings in the as-prepared condition and after aging at 100 ºC for 24 h and 72 h under static air at a heating rate of 10 ºC.min^{-1}: a) $T_{1.0}$; b) $T_{2.0}$.

From the DSC curves shown in Fig. 4a it is seen that the $T_{1.0}$ coating presented a wide endothermic peak near 330 ºC in the as-prepared condition. There is another small endothermic peak at 270 ºC. For the aged samples, both peaks appear at progressively smaller temperatures, suggesting that the onset of degradation processes was facilitated after aging. There was a small increase of the main peak area with aging, indicating that the $T_{1.0}$ is only slightly susceptible to physical aging.

The thermograms obtained for the $T_{2.0}$ coating (Fig. 4b) present the same basic characteristics of those observed for the $T_{1.0}$ coating. There is one major endothermic peak and a smaller one at lower temperatures for the as-prepared film. One interesting finding is that the position of the main endothermic peak is shifted to a higher temperature (345 ºC) in comparison with the $T_{1.0}$ coating (330 ºC). Another different characteristic is that the major peak is sharper in the thermogram of the $T_{2.0}$ coating whereas it is wider for the $T_{1.0}$ film. This suggests that the $T_{2.0}$ coating is more crystalline than the $T_{1.0}$ coating, probably due to high crosslink density resulting from the higher NCO/OH ratio. Both characteristics indicate that the $T_{2.0}$ coating has a higher thermal stability than the $T_{1.0}$ coating. This behavior was expected due to the higher NCO/OH ratio of the $T_{2.0}$ film which should improve the thermal stability of the organic material [32]. For the aged samples, the position of the major peak was shifted to lower temperatures, as occurred with the $T_{1.0}$ film. The area of this peak did not increase with the aging time, suggesting that it is not prone to physical aging. However, as the aging time increased the peak became wider and occurred at lower temperatures, indicating that the $T_{2.0}$ coating was more susceptible to degradation after aging.

The results obtained by DSC indicate that the $T_{2.0}$ coating is less prone to physical aging than the $T_{1.0}$ coating. This confirms the results obtained by positron annihilation spectroscopy and agrees with the literature [24], evidencing the importance of the NCO/OH ratio to the physical aging behavior of the polyurethane-urea coatings.

3.4 EIS measurements

Bode plots (impedance modulus vs. frequency) of the $T_{1.0}$ and $T_{2.0}$ films immersed in naturally aerated 3.5 wt.% NaCl solution at room temperature are shown in Fig. 5 for selected periods of immersion. Low values of the impedance modulus at the lowest frequencies are associated with organic coatings with poor protective properties [34]. Coatings with impedance modulus above 10^7 Ω.cm^2 at low frequencies are considered to have good corrosion protection ability [35]. The impedance behavior of highly protective coatings typically yields a plot (Z modulus vs. frequency) which gives a straight line with slope -1. When the slope deviates from this behavior at low frequencies, the coating assumes a more resistive behavior which is indicative of loss of its anticorrosion performance [36]. From the results shown in Fig. 5 one can observe that the impedance values of both coatings did not present a significant decrease with the immersion time. This reflects a good corrosion performance [37] independently of the NCO/OH ratio. Nevertheless, it is possible to notice that the $T_{2.0}$ coating presented higher impedance modulus than the $T_{1.0}$ coating. This behavior is more pronounced up to first 10 days of immersion but it is still observed after 42 days, although the difference between both coatings has been clearly diminished. It is also interesting to note the deviation from the pure

capacitive response of the $T_{1.0}$ coatings after 1 and 10 days of immersion, denoted by the change of negative slope at the lowest frequencies.

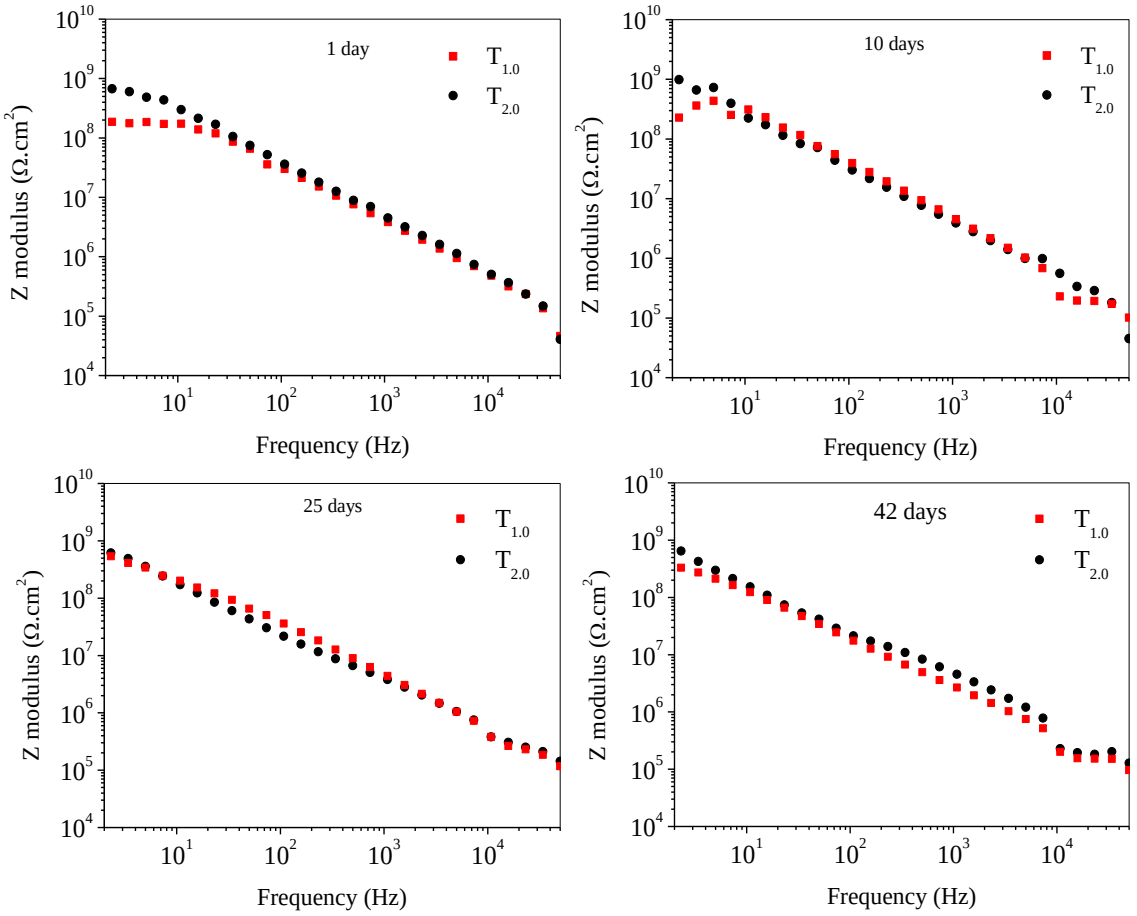

Figure 5. Bode plots (impedance modulus vs. frequency) of the $T_{1.0}$ and $T_{2.0}$ coatings immersed in naturally aerated 3.5 wt.% NaCl solution at room temperature for selected periods of immersion.

This suggests loss of corrosion protection ability for the $T_{1.0}$ coating whereas the $T_{2.0}$ coating maintained its almost pure capacitive response during the whole test. The slightly better response of the $T_{2.0}$ coating can be explained due to its higher NCO/OH ratio. The hydrophobicity of polyurethane-based coatings should increase with the NCO/OH [38]. Thus, high NCO/OH films should resist more to the penetration of water. This, in turn, would lead to good barrier properties and improved corrosion resistance.

The evolution of capacitance with the immersion time can be used to evaluate the performance of organic coatings owing to water uptake and formation of defects due to delamination. An increase of the coating capacitance is related to penetration of water, oxygen and ions through the coating [39]. Thus, this can give valuable information about the corrosion resistance of organic coatings. The evolution of capacitance with immersion time for the $T_{2.0}$ and $T_{1.0}$ coatings is shown in Fig. 6. The capacitance values were determined according to the procedure described in section 2.3.4.

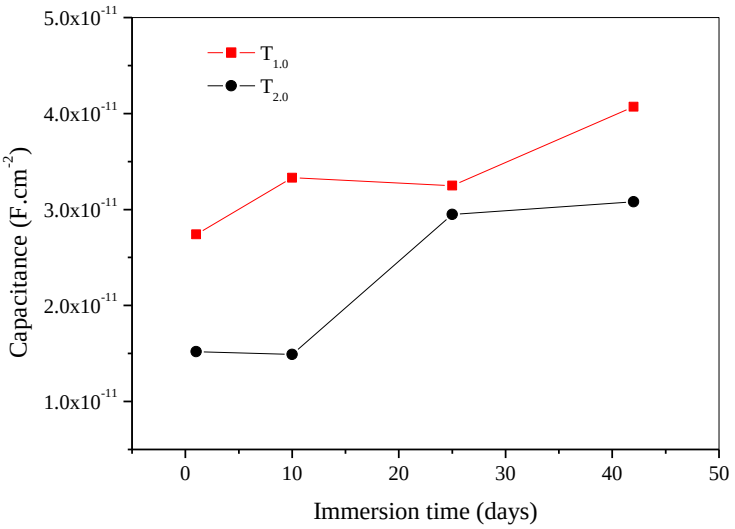

Figure 6. Capacitance evolution with immersion time in 3.5 wt.% NaCl solution at room temperature.

The magnitude of the capacitance for both coatings is typical of highly protective films [24,26]. The $T_{1.0}$ coating presented higher capacitance values than the $T_{2.0}$ coating independently of the immersion time. However, it is seen that this difference decreased for longer periods. The general trend for both coatings is that the capacitance increases with time, indicating that they are not immune to the testing environment. Yet, due to comparatively higher capacitance values, it is suggested that the $T_{2.0}$ coating has better barrier properties than the $T_{1.0}$ coating. This result confirms those shown in Fig. 5.

It is important to compare the results obtained by positron annihilation spectroscopy and DSC measurements regarding the physical aging behavior of the polyurethane-urea hybrid coatings with those obtained with EIS. In this regard, the physical aging susceptibility of the $T_{2.0}$ and $T_{1.0}$ was found to be similar, with a slightly better resistance of the $T_{2.0}$ film. From the EIS results, it is possible to infer that both coatings presented high corrosion resistance. However, the $T_{2.0}$ film was found to be less prone to water uptake due to its higher impedance modulus and lower capacitance values. Thus, positron annihilation spectroscopy, DSC and EIS results are in good agreement. The different NCOH/OH ratios of the coatings led to small but detectable differences in their degradation behavior by physical aging and corrosion. These techniques proved to be very sensitive to both the physical aging and corrosion phenomena of the polyurethane-urea hybrid coatings prepared in this work.

4. CONCLUSIONS

Positron annihilation spectroscopy was successfully employed to study the physical aging behavior of polyurethane-urea hybrid coatings. The results revealed that the coating with the highest NCO/OH ratio ($T_{2.0}$) provided the best performance against deterioration by physical aging. However,

both $T_{2.0}$ and $T_{1.0}$ films can be considered only little affected by physical aging according to the experimental procedure conducted in this work. DSC measurements confirmed the results obtained by positron annihilation spectroscopy. EIS data showed that the coatings were corrosion resistant, independently of the NCO/OH ratio. However, the best corrosion protection ability was observed for the $T_{2.0}$ coating. This corroborates the results obtained by positron annihilation spectroscopy and DSC. Physical aging susceptibility and corrosion resistance were directly related for the coatings investigated in the present work.

ACKNOWLEDGMENTS
The authors are thankful to the Brazilian agency FAPESP (Proc. 04/08893-5) for the financial support to this work. Dr. Otaviano A.M. Helene from University of São Paulo (LAL-IFUSP) is kindly acknowledged for his valuable help with the positron annihilation measurements.

References

1. F. Deflorian, S. Rossi, M. Fedel, *Corros. Sci.*, 50 (2008) 2360.
2. G. Grundmeier, W. Schmidt, M. Stratmann, *Electrochim. Acta*, 45 (2000) 2515.
3. M. Stratmann, R. Feser, A. Leng, *Electrochim. Acta*, 39 (1994) 1207.
4. Y. González-García, S. González, R.M. Souto, *Corros. Sci*., 49 (2007) 3514.
5. E. McCafferty, *Introduction to Corrosion Science*, Springer, New York, 2010.
6. A. Amirudin, D. Thierry, *Prog. Org. Coat.*, 26 (1995) 1.
7. M.E. Orazem, B. Tribollet, *Electrochemical Impedance Spectroscopy*, John Wiley & Sons, Inc., Hoboken, New Jersey, 2008.
8. X. Liu, J. Xiong, Y. Lv, Y. Zuo, *Prog. Org. Coat.*, 64 (2009) 497.
9. S. Shreepathi, P. Bajaj, B.P. Mallik, *Electrochim. Acta*, 55 (2010) 5129.
10. A. Xu, F. Zhang, B. Luo, F. Jin, T. Zhang, *Int. J. Electrochem. Sci.*, 8 (2013) 773.
11. Y.C. Jean, H. Chen, R. Zhang, Y. Li, J. Zhang, *Prog. Org. Coat.*, 52 (2005) 1.
12. R. Zhang, P.E. Mallon, H. Chen, C.M. Huang, J. Zhang, Y. Li, Y. Wu, T.C. Sandreczki, Y.C. Jean, *Prog. Org. Coat.*, 42 (2001) 244.
13. H. Leidheiser Jr., C. Szeles, A. Vértes, *Nucl. Intrum. Methods Phys. Res., Sect. A*, 255 (1987) 606.
14. R.C. MacQueen, R.D. Granata, *Prog. Org. Coat.*, 28 (1996) 97.
15. D.Y. Perera, *Prog. Org. Coat.*, 47 (2003) 61.
16. S. Montserrat, Y. Calventus, J.M. Hutchinson, *Prog. Org. Coat.*, 55 (2006) 35.
17. J.T. Garrett, J. Runt, J.S. Lin, *Macromolecules*, 33 (2000) 6353.
18. J.M. Sanchez-Amaya, R.M. Osuna, M. Bethencourt, F.J. Botana, *Prog. Org. Coat.*, 60 (2007) 248.
19. H. Renz, B. Bruchmann, *Prog. Org. Coat.*, 43 (2001) 32.
20. M.I. Aranguren, N.E. Marcovich, W. Salgueiro, A. Somoza, *Polym. Test.*, 32 (2013) 115.
21. R. Zhang, H. Cao, H.M. Chen, P. Mallon, T.C. Sandreczki, J.R. Richardson, Y.C. Jean, B. Nielsen, R. Suzuki, T. Ohdaira, *Rad. Phys. Chem.*, 58 (2000) 639.
22. E. do Nascimento, O. Helene, C. Takiya, V.R. Vanin, *Nucl. Instrum. Phys. Res., Sect. A*, 538 (2005) 723.
23. H. Chen, Q. Peng, Y.Y. Huang, R. Zhang, P.E. Mallon, J. Zhang, Y. Li, Y. Wu, J.R. Richardson, T.C. Sandrecki, Y.C. Jean, R. Suzuki, T. Ohdaira, *Appl. Surf. Sci.*, 194 (2002) 168.
24. M.C.L. De Oliveira, R.A. Antunes, I. Costa, *Int. J. Electrochem. Sci.*, 8 (2013) 4679.
25. C. Moreno, S. Hernández, J.J. Santana, J. González-Guzmán, R.M. Souto, S. González, *Int. J. Electrochem. Sci.*, 7 (2012) 8444.
26. A.S.L. Castela, A.M. Simões, M.G.S. Ferreira, *Prog. Org. Coat.*, 38 (2000) 1.

27. C.-W. Peng, C.-H. Hsu, K.-H. Lin, P.-L. Li, M.-F. Hsieh, Y. Wei, J.-M. Yeh, Y.-H. Yu, *Electrochim. Acta*, 58 (2011) 614.
28. S. Zhang, Z. Ren, S. He, Y. Zhu, C. Zhu, *Spectrochim. Acta, Part A*, 66 (2007) 188.
29. M.R. Patel, J.M. Shukla, N.K. Patel, K.H. Patel, *Mater. Res.*, 12 (2009) 385.
30. H. Cao, R. Zhang, C.S. Sundar, J.-P. Yuan, Y. He, T.C. Sandreczki, Y.C. Jean, *Macromolecules*, 31 (1998) 6627.
31. H. Cao, Y. He, R. Zhang, J.-P. Yuan, T.C. Sandreczki, Y.C. Jean, B. Nielsen, *J. Polym. Sci.: Polym. Phys.*, 37 (1999) 1289.
32. V. García-Pacios, V. Costa, M. Colera, J.M. Martín-Martínez, *Prog. Org. Coat.*, 71 (2011) 136.
33. R. van der Linde, E.G. Belder, D.Y. Perera, *Prog. Org. Coat.* 40 (2000) 215.
34. Q. Le Thu, G.P. Bierwagen, S. Touzain, *Prog. Org. Coat.*, 42 (2001) 179.
35. M. Zubielewicz, W. Gnot, *Prog. Org. Coat.*, 49 (2004) 358.
36. U. Rammelt, G. Reinhard, *Prog. Org. Coat.*, 24 (1994) 309.
37. J. Hu, X. Li, J. Gao, Q. Zhao, *Prog. Org. Coat.*, 65 (2009) 504.
38. E.-S.M. Negim, L. Bekbayeva, G.A. Mun, Z.A. Abilov, M.I. Saleh, *World Appl. Sci. J.*, 14 (2011) 402.
39. C. Corfias, N. Pébère, C. Lacabanne, *Corros. Sci.*, 41 (1999) 1539.